TOPICAL REVIEW — 2D materials: physics and device applications

Light–matter interaction of 2D materials: Physics and device applications*

Zi-Wei Li(李梓维)[1,2], Yi-Han Hu(胡义涵)[1], Yu Li(李瑜)[1,2], and Zhe-Yu Fang(方哲宇)[1,2,3,†]

[1] School of Physics, State Key Laboratory for Mesoscopic Physics, Peking University, Beijing 100871, China
[2] Academy for Advanced Interdisciplinary Studies, Peking University, Beijing 100871, China
[3] Collaborative Innovation Center of Quantum Matter, Beijing 100871, China

(Received 29 August 2016; revised manuscript received 17 October 2016; published online 18 January 2017)

In the last decade, the rise of two-dimensional (2D) materials has attracted a tremendous amount of interest for the entire field of photonics and opto-electronics. The mechanism of light–matter interaction in 2D materials challenges the knowledge of materials physics, which drives the rapid development of materials synthesis and device applications. 2D materials coupled with plasmonic effects show impressive optical characteristics, involving efficient charge transfer, plasmonic hot electrons doping, enhanced light-emitting, and ultrasensitive photodetection. Here, we briefly review the recent remarkable progress of 2D materials, mainly on graphene and transition metal dichalcogenides, focusing on their tunable optical properties and improved opto-electronic devices with plasmonic effects. The mechanism of plasmon enhanced light–matter interaction in 2D materials is elaborated in detail, and the state-of-the-art of device applications is comprehensively described. In the future, the field of 2D materials holds great promise as an important platform for materials science and opto-electronic engineering, enabling an emerging interdisciplinary research field spanning from clean energy to information technology.

Keywords: 2D materials, light–matter interaction, 2D optoelectronic devices, surface plasmon

PACS: 68.65.–k, 63.20.kk, 85.60.–q, 73.20.Mf **DOI:** 10.1088/1674-1056/26/3/036802

1. Introduction

Since graphene was first successfully exfoliated from graphite in 2004,[1] great attention and efforts have been devoted to two-dimensional (2D) materials. With the development and innovation of growth technology, more and more 2D materials have been discovered and synthesized so far.[2,3] The chemical vapor deposition (CVD) methods gradually replace the mechanical exfoliation, which can provide large-area single crystal films with high quality.[4,5] These atomic thin materials with the breakthrough of integration technologies accelerate the on-chip device applications in fields of sensing, communications, and photodetection.[6]

The group of 2D materials is a big family, involving graphene, graphene oxide (GO), hexagon boron nitride (h-BN), and transition metal dichalcogenides (TMDs).[7–9] Because of their extraordinary electronic, optical, and mechanical properties, 2D materials hold huge potential for applications in nano-photonic and opto-electronic devices. Notably, the electronic mobility of graphene is extraordinarily high ($>$ 100000 $cm^2 \cdot V^{-1} \cdot s^{-1}$) due to the ballistic transport of charge carriers, performing 100 times faster than Si transistors.[10] Currently, the fastest graphene transistor was reported in 2010 showing 300 GHz cut-off frequency.[11] In addition, the electronic energy band of 2D materials is strongly influenced by the number of 2D layers. For example, when bulk MoS_2 is thinned to monolayer structure, it transforms from an indirect to a direct gap semiconductor.[12,13] Besides, MoS_2 monolayer has strong exciton photoluminescence (PL) at room temperature due to its tightly bound exciton with remarkable binding energy ($>$ 500 meV).[14–16] Moreover, the 2D films are also known as "ultra-strength materials" with high mechanical elasticity (strained over 125%) and Young's modulus, which are utilized to produce high-performance flexible opto-electronic devices with organic materials.[17–20]

In this paper, we briefly review the recent progress of 2D materials in optical properties, and enhanced optical and opto-electronic performance based on plasmonic effects. Initially, we will discuss the fundamental optical properties of 2D materials and their inherent weakness in poor optical cross-section. Graphene and MoS_2 are typical candidates to study the physics on light–matter interaction, including optical absorption, excitonic PL, and surface plasmon of 2D materials. Additionally, we outline the mechanism of plasmon enhanced light–matter interaction of 2D materials, and the state-of-the-art plasmon-coupled 2D devices. Their PL and absorption can be dramatically enhanced by the effect of plasmonic hot electrons

*Project supported by the National Basic Research Program of China (Grant No. 2015CB932403), the National Natural Science Foundation of China (Grant Nos. 61422501, 11674012, 11374023, and 61521004), Beijing Natural Science Foundation, China (Grant No. L140007), Foundation for the Author of National Excellent Doctoral Dissertation of China (Grant No. 201420), and National Program for Support of Top-notch Young Professionals, China.

†Corresponding author. E-mail: zhyfang@pku.edu.cn

© 2017 Chinese Physical Society and IOP Publishing Ltd

doping and near-field enhancement. 2D materials perform ultrafast and ultrasensitive photoresponse with plasmonic structures, which can be further applied in a large spectral range from UV to near-infrared. Finally, we highlight the properties and advantages of 2D devices for a wide variety of applications among photocatalysis, photo-thermo, and light-emitting.

2. Light–matter interaction in 2D materials

2.1. Optical absorption of 2D materials

2D materials show unique optical properties, such as large optical cross-section and high transmittance, which are suitable for transparent electrodes and opto-electronic device applications.[21–23] Graphene can be optically observed from the color contrast on top of a SiO_2/Si substrate, despite being a single atom sheet with a form of hexagonal carbon lattice, as shown in Fig. 1(a).[24] The color contrast of graphene can be adjusted by changing the SiO_2 thickness and switching the illumination wavelength.[25] Graphene has a linear dispersion in electronic structure, and it is defined as a "semi-metal" material because of its zero band gap. The transmittance (T) of a freestanding single-layer graphene can be expressed in terms of the fine-structure constant α as $T=(1+0.5\pi\alpha)^{-2}\approx 1-\pi\alpha\approx 97.7\%$, where $\alpha=e^2/(4\pi\varepsilon_0\hbar c)=G_0/(\pi\varepsilon_0 c)\approx 1/137$, and the fixed universal optical conductance is $G_0=e^2/4\hbar\approx 6.08\times 10^{-5}\ \Omega^{-1}$.[26] A graphene sheet only reflects $<0.1\%$ of the incident light in the visible region, and only absorbs over 2.3% of the visible spectral range. The absorption spectrum of graphene is quite flat from 300 nm to 2500 nm with a main absorption peak in the ultraviolet region ($\sim$ 270 nm), which is due to the interband transition of the electrons.[27] It is reported when a graphene layer is patterned into an array of closely packed graphene nanodisks, the optical absorption of graphene can be increased to above 30% at resonance frequencies in the infrared range.[28,29] The absorption enhancement can be actively tuned by changing the nanodisk size, gate voltage, and interparticle spacing. Cutting graphene into nanostructures can modulate the resonant absorption, which possesses great potential for near-infrared and infrared optoelectronic applications.

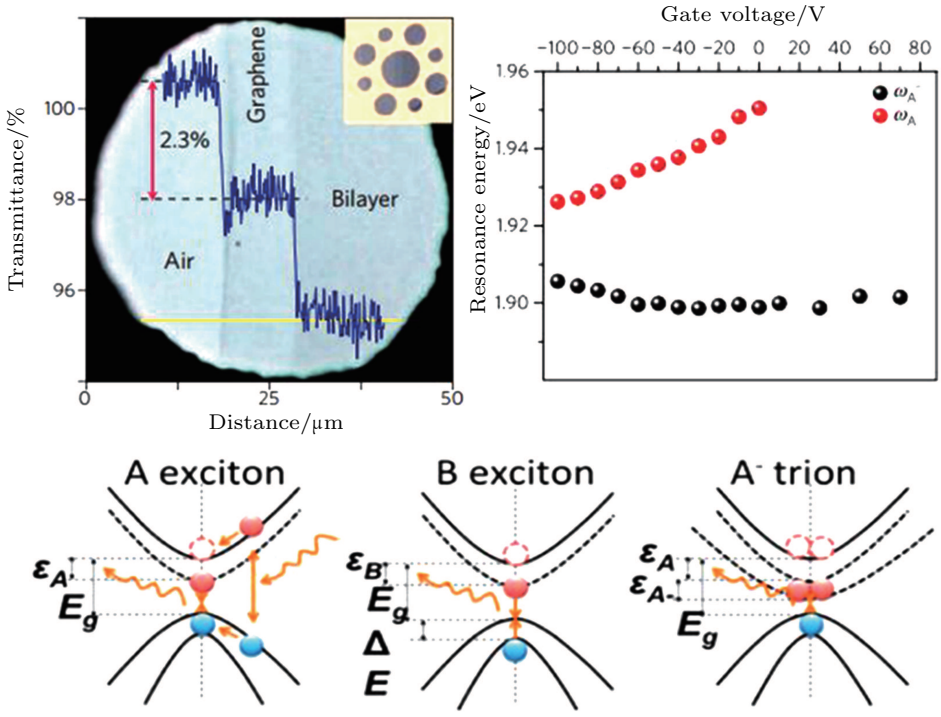


Fig. 1. (color online) The optical properties of 2D materials. (a) Optical image of single layer graphene and bilayer graphene.[24] (b) Multi-exciton transformation of MoS_2 monolayer with electric gate doping.[15] (c) The schematic view of optical absorption, exciton and trion formation in TMDs.[32]

The direct band gap semiconductor is an ideal candidate for light-emitting devices due to the direct electron transition without the loss of momentum. MoS_2 monolayer is widely known as an n-type semiconductor, which is caused by intrinsic sulfur vacancy defects.[30] In a monolayer film, Mo atoms are sandwiched between two-layered S atoms with a height of 0.65 nm. Their atomic thickness strengthens the interaction of exciton and charge carriers, forming tightly bound charge excitons, namely, trion.[31] When applying back gate voltages on a monolayer MoS_2 transistor, the absorption spectra show obvious tuning with variant gate biases as shown in Fig. 1(b).[15] The absorption peak at -80 V is dominated by neutral exciton A and trion A-. Trion A- consists of one hole of up-spin and two electrons of opposite spins. As the negative gate voltage

decreases, exciton A is sensitive with doping charge carriers, resulting in a spectral evolution. When the voltage is increased to 0 V, it is hard to track the peak position, and even up to +70 V, the spectrum is completely dominated by trion A-.

Figure 1(c) shows the schematic view of light–matter interaction in MoS_2 monolayer.[32,33] In the valley of direct band gap, free electrons and holes generated by illumination cool down to the extreme points of the conduction band and valence band separately, and form an exciton at a lower exciton energy level (dotted line in Fig. 1(c)). There are three characteristic absorption peaks of MoS_2 monolayer, involving exciton A, exciton B, and trion A-. Their energies can be expressed as $PL_A = E_g - \varepsilon_A$, $PL_B = E_g + \Delta - \varepsilon_B$, and $PL_{A-} = E_g - \varepsilon_A - \varepsilon_{A-}$, where E_g is the direct band gap energy of single-layer MoS_2, Δ is the valence band splitting energy, and ε_A, ε_B, and ε_{A-} are the binding energies of exciton A, exciton B, and trion A-, respectively. The energy difference of exciton A and exciton B is arising from the valence band splitting at the K-point in the Brillioun zone originating from the spin–orbit coupling.[14] By theoretical prediction and experimental verification, the exciton binding energy of MoS_2 is determined to be as large as 500 meV, and the binding energy of the trion is about 20 meV at room temperature.[15] Besides, MoS_2 absorption spectra are closely related to the environment temperature.[34] Exciton and trion both redshift as the temperature increases, which is attributed to the temperature-induced variation of lattice parameters. In addition, exciton and trion spectra broaden as the temperature increases and become almost indistinguishable above 230 K. This temperature-dependent broadening is attributed to the increase of the scattering rates.

2.2. Optical emission of 2D materials

PL study has been extensively used to probe radiative recombination and the emission properties of 2D materials. Although graphene is a zero band gap semi-metal, the ultrafast laser pulse can generate a large number of non-equilibrium carriers, resulting in hot photons.[35,36] Besides, the luminescence of graphene could also be realized by inducing a band gap, such as cutting it into graphene quantum dots (GQDs),[37] or other chemical and physical treatments.[38,39] By far, the PL of graphene-based materials has been extensively produced covering the ultraviolet, visible, and infrared spectral range.[40] It has been widely reported that the GQDs can be prepared by top-down and bottom-up methods.[41] Notably, the PL mechanism of GQDs is unclear but certainly related with the quantum effect. It is reported that PL of GQDs can be modulated by changing the structure size, edge state, concentration, and pH of solution, as shown in Fig. 2(a). However, the PL efficiency of individual GQDs is still a great challenge for practical applications. Some graphene oxides with an opening band gap emit PL with a broad spectral lineshape. In Fig. 2(b), it is reported that single layer graphene flakes can shine bright luminescence via mild oxygen plasma treatment, which is associated with oxygen-related defect states.[38]

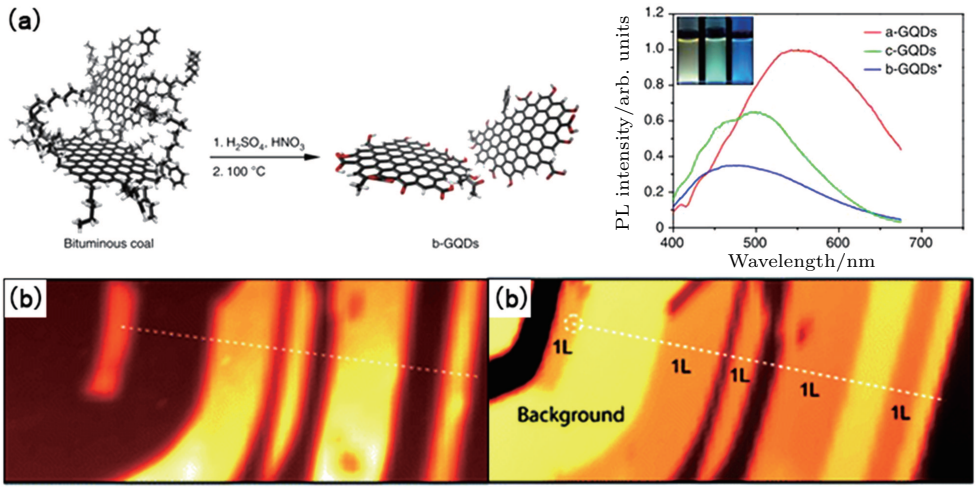


Fig. 2. (color online) Light emission of graphene. (a) PL of graphene quantum dots fabricated by "top-down" method.[37] (b) Graphene shine luminescence via mild oxygen plasma treatment.[38]

MoS_2, as a member of TMDs family, performs highly efficient and multi-exciton PL in the monolayer regime, although its bulk material is an indirect band gap semiconductor with negligible photoluminescence.[12,13,33] PL properties of MoS_2 are varied with the layer number and environmental temperature. By measuring MoS_2 PL spectra with layer number N = 1–6, the direct band gap of materials at the K-point does not change with the layers, but the direct exciton transition at the K-point gives different quantum efficiencies for monolayer and few layers.[14] With increasing laser power from 200 μW to 40 mW at 4 K, it is found that the variation of total integrated intensity of exciton A and B is linear with the laser power. The PL peaks broaden and redshift as the temperature increases from 4 K to 300 K.[42]

In addition, MoS_2 PL intensity and peak energy can be modulated in the charge doping process, involving physical and chemical methods. The electrical gating of PL and optical absorption in MoS_2 monolayer has been investigated.[43] When the gate voltage is decreased from +50 V to −50 V, a hundred-fold enhancement in PL intensity is observed, but the peak energy remains nearly constant. In Fig. 3(a), it shows the report of strong PL enhancement of MoS_2, as high as thousands-fold, which is arising from defect engineering and oxygen bonding.[44] Such a huge PL enhancement is attributed to oxygen bonding induced heavy p-doping, as well as high quantum efficiency of exciton localized at defect sites. The chemically adsorbed oxygen provides a much more effective charge transfer (0.997 electrons per O_2) compared with the physically adsorbed oxygen.

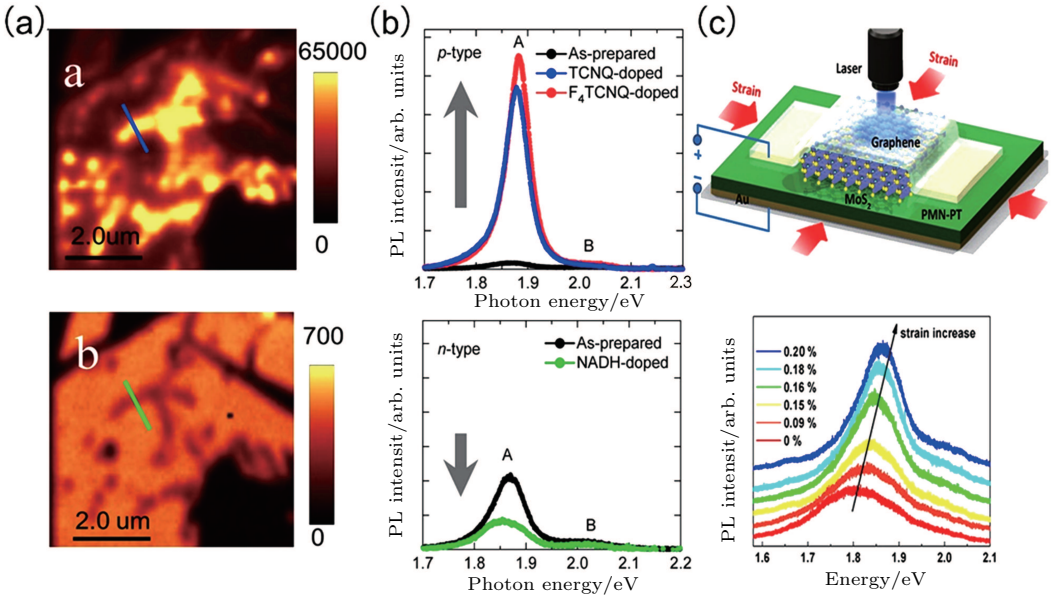


Fig. 3. (color online) PL tuning of MoS_2 monolayer. (a) Defect engineering and oxygen bonding enhancing MoS_2 PL.[43] (b) Chemical molecules interaction tuning MoS_2 PL.[45] (c) Mechanical strain induced MoS_2 PL changing.[18]

In Fig. 3(b), it has been reported that the tunable PL properties of MoS_2 monolayer can be realized by using the chemical doping technique.[45] The PL intensity of MoS_2 monolayer is drastically enhanced by the adsorption of p-type dopants (F4TCNQ and TCNQ). Inversely, the PL signal is reduced by the adsorption of n-type dopants (NADH). These PL modulations result from the switching of exciton and trion PL contribution depending on the charge density of MoS_2. The doping electron density in the procedure of this chemical interaction is estimated as 5.8×10^{13} cm^{-2}. As shown in Fig. 3(c), a novel electromechanical device with controllable biaxial compressive strain has been reported to modulate MoS_2 PL. The PL spectra can be increased up to 200% with a 40% reduction in the full-width for an applied strain of $\sim 0.2\%$.[18]

2.3. Surface plasmon of 2D materials

Surface plasmon is the collective oscillation of free electrons in the metal and 2D materials, which can concentrate light into electron propagation behaviors using subwavelength structures.[46] Also, optical properties of 2D materials can be actively controlled by controlling electronic doping.[16,47] In physics, the principle of surface plasmon can be understood by the repeating transition of free electrons near the Fermi level of materials. When structures are excited by light, the oscillating electromagnetic field acts as the applied force, driving the electrons surrounding the positive nuclei periodically along the field direction. Meanwhile, the Coulombic attraction performs as the restoring force pulling the electrons back. According to the propagation length, the surface plasmon can be divided into two types, one is the localized surface plasmon (LSP), and the other is the surface plasmon polaritons (SPPs).[48–51] Both effects in metal nanostructures and nanoparticles have been investigated widely for several decades, which has developed a class of applications for super-resolution imaging, efficient energy harvesting, near-field imaging and sensing. Here, we briefly introduce the plasmonic effects derived from 2D materials and their nanostructures, which has been developed into an emerging interdisciplinary research field in recent years.

In 2012, the experimental phenomena of surface plasmon propagation in single layer graphene has been first reported, as shown in Fig. 4(a).[52] By fabricating tapered graphene ribbon on SiC substrate, the propagating surface plasmons were lauched and detected using near-field scattering microscopy

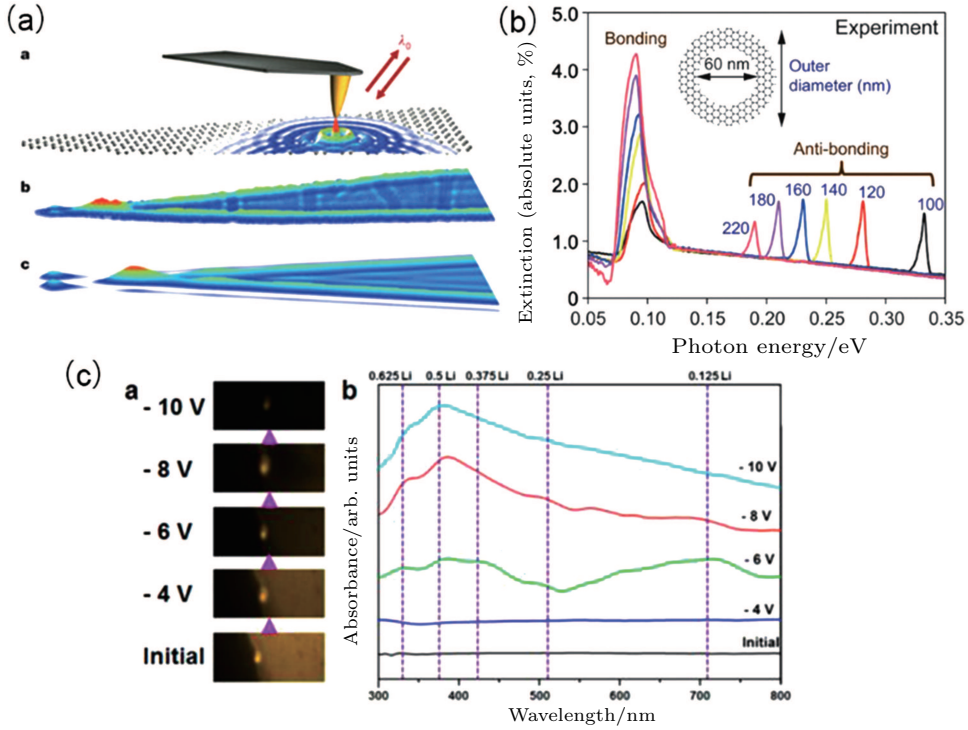


Fig. 4. (color online) Surface plasmon of graphene and MoS_2. (a) Gate-tunable surface plasmon polariton of graphene nano-ribbon.[52] (b) Size-dependent localized surface plasmon of graphene nano-ring structures.[28] (c) Plasmon resonance of highly doped MoS_2.[54]

with infrared light excitation. The plasmon modes and their associated optical signals of graphene can be tuned electrically by gate doping, which changes the concentration of charge carriers and the Fermi level of graphene. The observed plasmon wavelength is more than 40 times smaller than the excitation wavelength.

An alternative way to open the gap of graphene is patterning graphene nanostructures. The absorption phenomena of graphene nanostructures are associated with plasmon resonance, which is flexibly controlled by changing the shape and size of graphene nanostructures. In Fig. 4(b), it is reported that absorption spectra of graphene nanostructures can be controlled by tailoring the plasmon resonance of nanostructures, via both gate doping and plasmon hybridization.[28,29] Their Fermi level variation enables the fast control of the plasmon wavelength, whereas changing the structure parameter allows us to operate the antibonding modes of narrow rings at a wavelength of 3.7 μm. This approach can be extensively utilized to yield tunable plasmons in the near-infrared or even in the visible range.

The density of electrons in pristine MoS_2 monolayer is about 10^{13} cm^{-2}, which is much lower than that of graphene and other metal materials, hence it is really hard to observe the surface plasmon resonance of MoS_2 monolayer in the visible spectral range.[53] In Fig. 4(c), it is reported that MoS_2 plasmon resonance can be observed in the visible and near UV wavelength by electrochemically injecting lithium into MoS_2 nanoflakes.[54] These plasmon resonances are activated and controlled by the electrochemical force induced heavy doping, which contributes to the formation of the semi-metal state of Li_xMoS_2.

3. Plasmon-coupled 2D materials and devices

3.1. Plasmon enhanced light–matter interaction

The interplay of surface plasmon and emitters has been extensively reported, involving dye molecules and quantum dots. However, the influence of plasmon enhanced light–matter interaction has not been concluded in the materials system of 2D materials. The mechanism of plasmon enhanced light–matter interaction can be understood in the following several aspects: enhanced light scattering, strengthened near-field intensity, plasmonic hot electrons doping, and strong coupling.

The metallic nanoparticles and nanostructures will absorb and scatter light signals due to their dielectric constant in physical nature. In Fig. 5(a), small particles act as a light scattering source in the near field distance, and the light path can be increased resulting in enhanced light–matter interaction.[55] This enhancement effect is usually weak in the practical applications. The resonant absorption of surface plasmon will generate huge field enhancement, especially for smaller mode volumes, and the radiative properties of exciton in TMDs can be dramatically modified. In quantum-electrodynamic theory, exciton recombination is treated as a dipole emission, and its photonic local density of states can be modified by the environmental electromagnetic field. If the exciton energy is

overlapped with the surface plasmon resonant (SPR) energy, the excitonic radiative decay rates are dramatically enhanced, leading to improved quantum yield. Particularly, the position and orientation of the dipole emitter play a significant role in PL enhancement of TMDs.[56] Besides, the effective cross section of metallic nanostructures is even bigger than their geometric size, which means that the SPR induced field performs as an objective lens with high numerical aperture collecting more emission signal into free space.[57]

The damping process of SPR can generate radiative photon or non-radiative hot electron–hole pairs via Landau damping. First, hot electrons are generated in the metal due to photon absorption, then move towards the metal/semiconductor interface. For example, if the energy of hot electrons is larger than the Schottky barrier energy of TMDs, the hot electrons will jump through and inject into TMDs as free carriers, leading to the change of dielectric constant and photocurrent. In spectral characterization as shown in Fig. 5(b), TMDs' PL shifting and intensity attenuation are mostly related with hot electrons doping effects during an ultrafast process.[58] Even, the energy level occupation of hot electrons will induce phase transition of TMDs at low temperature.[59] In addition, the coupling strength is important for the hybrid system of TMDs and plasmonic nanostructures. The strong coupling is determined by the relation between exciton and plasmon, where the average dissipation rate in the system is larger than the exciton–cavity energy exchange rate. Plasmonic lattice structures benefit both from the LSR induced field enhancement and high quality lattice modes, providing greater freedom for efficient manipulation of exciton–plasmon couple strength, as shown in Fig. 5(c). The splitting absorption spectra of TMDs with plasmonic nanostructures are attributed to the strong coupling effect.[60,61]

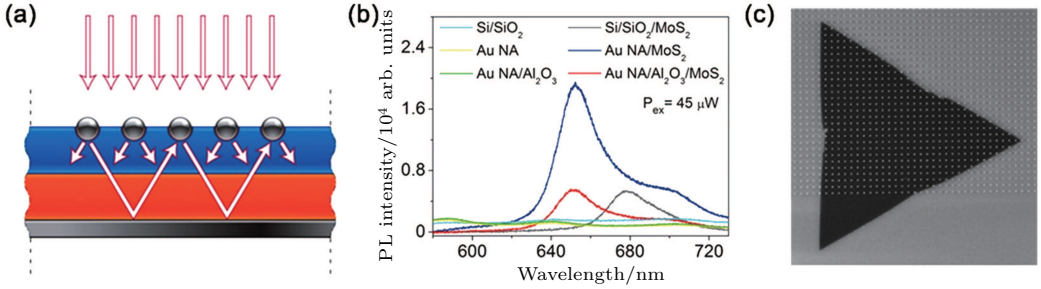


Fig. 5. (color online) The mechanism of plasmon enhanced light–matter interaction of 2D materials. (a) Metallic nanoparticles induced light scattering enhancement.[55] (b) Plasmonic hot electrons injection induced PL spectra tuning.[58] (c) Plasmonic lattice modes coupled with MoS_2 exciton resulting in strong coupling.[60]

3.2. Surface plasmon enhanced optical signals

The direct band gap luminescence of some 2D materials (i.e., MoS_2, h-BN, GO) is remarkable for the properties of strong exciton binding energy and high emission efficiency. However, the atomic thin thickness remains a great challenge for light–matter interaction, involving weak light absorption and poor PL efficiency, which limits their development and application in sensing and detecting devices. An alternative way to solve this problem could be constructing hybrid structures incorporating the plasmonic effect with 2D semiconductors. The origin of the enhancement effect is the localized electromagnetic field in the vicinity of the metal nanostructures, which is generated by the metallic plasmonic resonance effect. Some distinctive works on hybrid structures are presented to discuss the interaction of surface plasmon and exciton.

In Fig. 6(a), it is reported that MoS_2 absorption and PL can be actively controlled by depositing golden nanoparticles onto a MoS_2 monolayer, which shifts the exciton binding energy as large as 15 meV with increasing laser power.[16] In this plasmon-assisted process, plasmonic hot electrons are generated and transferred into MoS_2 flakes, resulting in n-type doping. The injected doping charges change the dielectric permittivity of materials and strengthen the exciton binding energy. This spectroscopic tuning is strongly associated with Au nanoparticle concentrations, excitation laser wavelengths, and laser intensities. The Drude model can be used to represent the effective permittivity with hot electrons doping, and the doping density can be estimated from the experiment data of binding energy changing. The contribution of the hot electrons doping effect is dominant in this work due to the strong absorption of 5 nm golden nanoparticles. In another work, the lattice mode of Ag nanodisks coupled with MoS_2 exciton showing tunable optical absorption, which can be elaborated in a two oscillator model.[62] Laser induced exciton population changing will affect the modes modulation of plasmonic lattices. The changing dielectric constant of MoS_2 can be expressed as the change of photoexcited exciton. These two works are totally different, the former is in the view of electronics, and the latter concentrates the topics on the photonics.

Typically, the PL enhancement of TMDs with metal nanostructures is usually around 100-fold. However, other group reported a giant PL enhancement of WSe_2, as high as 20000-fold[63] Figure 6(b) shows the SEM image of suspending WSe_2 flakes over sub-20-nm-wide trenches on a gold sub-

strate. The huge enhancement of PL intensity is attributed to the huge resonant absorption at 633 nm laser in a lateral gap, which efficiently boosts the light–matter interaction in WSe_2. The local confinement of electromagnetic field in deep trenches provides an effective way to obtain giant PL in TMDCs.

Figure 6(c) shows the schematic view of MoS_2 monolayer coupling with plasmonic nanocavity.[64] The silver nanocubes were fabricated onto golden film constructing nanocavities less than 15 nm. Two resonant modes can be tuned respectively, which provides a flexible and tunable plasmonic platform to control the optical process of 2D materials. Notably, a 2000-fold enhancement of MoS_2 PL is realized, which contributes in two ways, one is tailoring absorption enhancement at the first harmonic frequency, and the other is increasing PL efficiency at the primary resonance.

In addition to intensity enhancement, PL spectra of 2D materials influenced by the plasmonic effect also show peak broadening and energy shifting. In Fig. 6(d), it has been reported that the phase transition of MoS_2 can be observed in a vacuum chamber at 77 K. By combining Au nanoparticles with MoS_2 monolayer, plasmonic hot electrons transfer into MoS_2 flakes, inducing a transient and reversible phase transition from 2H to 1T.[59] The evidence for this phase transition is the appearance of characteristic Raman modes of the octahedral phase and a redshift change in the PL spectrum.

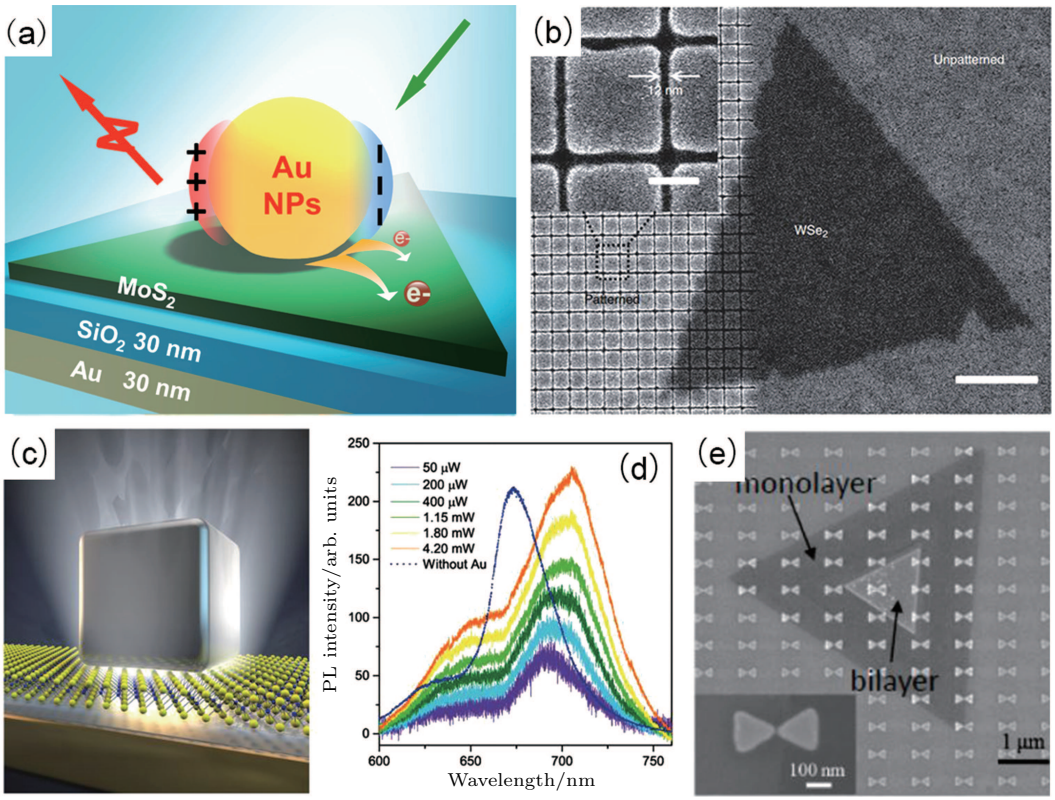


Fig. 6. (color online) Surface plasmon enhanced optical properties of 2D materials. (a) Plasmonic hot electrons doping of MoS_2 monolayer.[16] (b) Giant enhancement of WSe_2 PL by fabricating plasmonic trenches.[63] (c) Absorption and PL enhancement of MoS_2 by tailoring two plasmonic resonant modes of silver cube.[64] (d) Plasmonic hot electrons induced transient phase transition of MoS_2 monolayer.[59] (e) MoS_2 PL tuning by "bow-tie" structure induced Fano resonance.[67]

The Fano resonance in plasmonic nanostructures is the spectral interference between a narrow discrete resonance and a broad continuum state. Because their line shape and spectral position are very sensitive to small perturbations, it is quite attractive for a wide range of applications on sensing.[65,66] It is reported that MoS_2 spectra can be modulated by tuning the Fano resonance of a plasmonic bowtie, as shown in Fig. 6(e).[67] At 77 K, the MoS_2 exciton with a sharp resonance couples with broad plasmonic modes, giving rise to the Fano resonance, which can be tuned by altering the coupling strength via changing the structural parameters of the bowties lattice.

3.3. Surface plasmon enhanced photodetection

The optoelectronic devices based on 2D materials have a broad range of applications due to their outstanding electronic properties and unique optical properties. Plasmonic nanostructures play an important role in harvesting optical signals from UV via visible to near-infrared range, which help to convert light energy into photocurrent.[48,49] Figure 7 shows a few kinds of 2D materials photodetection with the plasmon-assisted enhancement effect.

Figure 7(a) is a sandwich graphene photodetector with plasmonic clusters integration.[68] The heptamer golden nanodisks are sandwiched between two graphene monolayers yielding a graphene-antenna photodetector, which performs an 800% enhancement of the photocurrent relative to the pristine graphene device. The plasmonic induced enhancement effect comes from two ways: one is due to the plasmonic hot electrons generation in the decay channel, the other is caused by the enhanced excitation of intrinsic graphene electrons. The sensitive absorption of the detector can be tailored by changing the structural geometry of the plasmonic clusters. The internal quantum efficiency of the device can be up to over 20% through the visible to near-infrared spectral range.

In a plasmon-coupled graphene photodetector, a maximum amplification enhancement of the photovoltage was observed more than 20 times by taking advantage of the strong field enhancement of the plasmonic nanostructures.[69] As shown in Fig. 7(b), the selective excitation of wavelength and polarization can be achieved by employing nanostructures with different geometries, such as stripes, nanodisks, and dimer disks. The photoresponse with polarized light depends on the resonant excitation of structure-dependent plasmonic modes, that is, the transverse polarization generates much stronger enhancement than the longitudinal polarization in stripe structures.

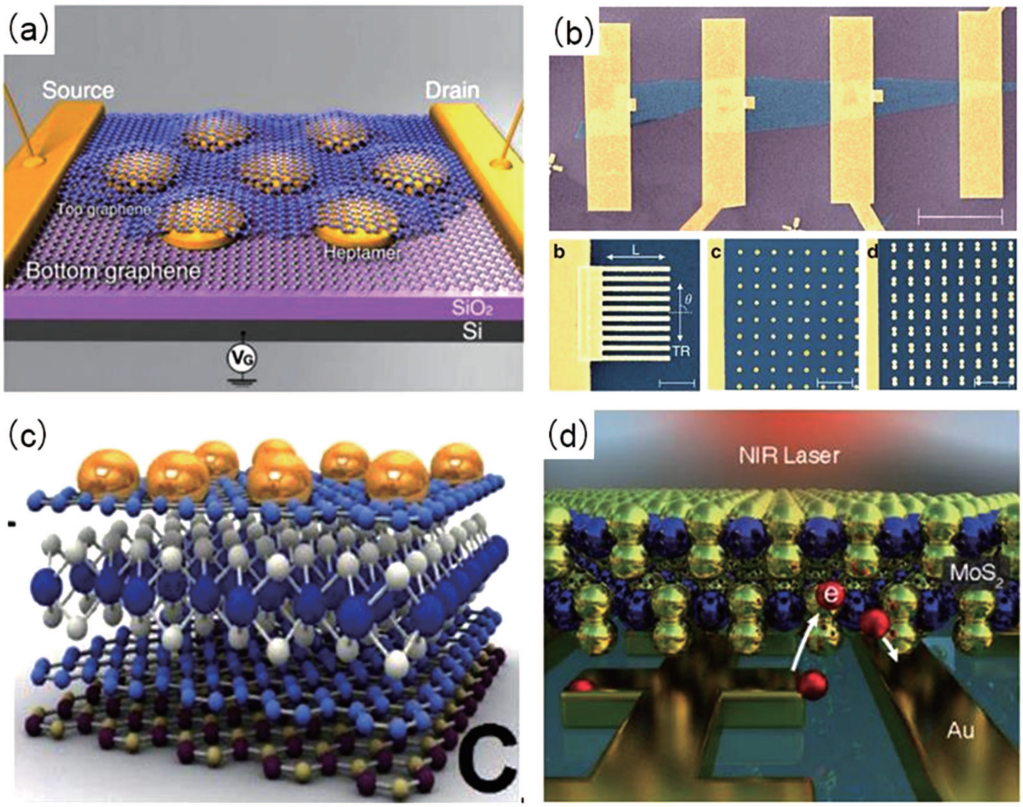


Fig. 7. (color online) Surface plasmon enhanced photodetection of 2D materials. (a) Plasmonic heptamer-antenna enhanced graphene sandwich photodetection.[68] (b) Plasmonic nanostructures enhanced graphene photodetection.[69] (c) Surface plasmon enhanced photodetection based on 2D heterostructure.[70] (d) Hot electron-based near-infrared photodetection of bilayer MoS_2.[7]

Figure 7(c) shows the plasmon-assisted photodetectors device based on vertical stacked 2D materials.[70] The device possesses an enhanced external quantum efficiency as high as 30%, which is arising from the strong light–matter interaction in these atomically thin layers. On a graphene/WS_2/graphene stacked 2D device, the Fermi level of the two graphene layers can be appropriately adjusted separately via gate electrostatic doping. Plasmonic nanospheres acting as optical resonators are further utilized to increase the photocurrent of h-BN/graphene/MoS_2/graphene heterostructures, where the optical field in the active layer is dramatically enhanced, allowing for a 10-fold increase in the photocurrent.

In Fig. 7(d), a bilayer MoS_2 photodetection with hot electron injection has been reported, which is designed in the near infrared range.[7] The designed nanostructures can generate plasmonic hot electrons jumping over the Schottky barrier of MoS_2/Au. A huge photo-gain as large as 105 times is obtained, and the photoresponsivity is 5.2 A/W at 1070 nm. The systematic investigations were performed to exclude other effects, including decay induced photo-thermo-electrical effect and traps induced photo-amplification effect. The device performance is much higher than silicon-based hot electron photodetectors, which reveals that 2D semiconducting TMDs present strong light–matter interaction resulting in large pho-

tocurrent production.

Other types of MoS_2 photodetections have also been investigated widely. It is reported that a three-fold enhancement of photocurrent has been achieved on few-layer MoS_2 with periodic Au nanoarrays.[71] And a dye-sensitized MoS_2 photodetector was realized by depositing rhodamine 6G (R6G).[72] The proposed photodetector shows a maximum photoresponsivity of 1.17 $A \cdot W^{-1}$ and a total effective quantum efficiency (EQE) of 280% at 520 nm. It is reported that the MoS_2 photodetection with copper phthalocyanine shows a photoresponsivity of ~ 1.98 $A \cdot W^{-1}$ and an external quantum efficiency of $\sim 12.57\%$.[73] Because TMDs possess inequivalent valleys in electronic band structures, the circular photogalvanic current of TMDs can be generated by switching linear polarized light to circular polarized light periodically. The magnitude and direction of this spin-coupled valley photocurrent can be further controlled by an external electric field.[74]

4. Other device applications of 2D materials

The interface problem has sparked wide interest, especially on a 2D material heterostructure stacked with van de Waals force.[23,75,76] Several works have been reported that the surface plasmon resonance of carbon dots and GQDs can be excited in the UV–visible range.[78,79] It is reported that an effective and active-controlled optical doping process can be realized by depositing GQDs solution onto MoS_2 monolayer, which induces the charge transfer at the interface of the GQD/MoS_2 heterostructure, as shown in Fig. 8(a).[80] The doping effect is induced by the charge tunneling of localized surface plasmon of GQDs, which is further used to modulate the degree of circular polarization of MoS_2 monolayers.

In the field of environmentally-friendly energy, 2D semiconductors hold great potential in photocatalytic hydrogen production. Plasmonic coupled MoS_2 enable better production of hydrogen due to their enhanced absorption and fast electron mobility. The illustration of hot-electron-assisted MoS_2 catalysis is shown in Fig. 8(b).[81] With plasmonic hot electron doping, the interface resistance between Au NPs and MoS_2 is reduced, and the photo-excited transient 1T phase of MoS_2 exhibits a better catalytic performance. The enhanced catalytic activity for plasmonic effects exhibits an accumulative behavior with each round of laser illumination from 0 to 25 mW.

Besides the doping effect, the absorption of surface plasmon also produces a localized thermo-effect heating the environment. It is reported that the photoluminescence emission of MoS_2 can be tailored by switching off- and in-resonance excitation of plasmonic nanorod, as shown in Fig. 8(c).[82] Using a temperature calibration procedure based on PL spectral characteristics, the local temperature distribution has been estimated. The temperature of plasmon-coupled MoS_2 is nearly four times higher than that of referenced MoS_2.

Photonic crystal cavities, with low loss and strong field restriction, can extremely enhance the light–matter interaction in the artificial structure. Figure 8(d) shows a nanoscale laser based on 2D quantum materials and the photonic cavity.[83] The novel laser is a low-threshold device, where WSe_2 monolayer is chosen as the gain medium due to its high PL efficiency in the visible range. An L3 type of photonic crystal cavity is prefabricated on a GaP thin membrane without absorption overlapping the WSe2 PL. The three missing holes in the photonic crystal play a significant role in enhancing the spontaneous emission efficiency, where the Q-factor is about 10^4 representing 40-fold enhancement. The temperature effect and reproducibility of the laser device are analyzed in detail,

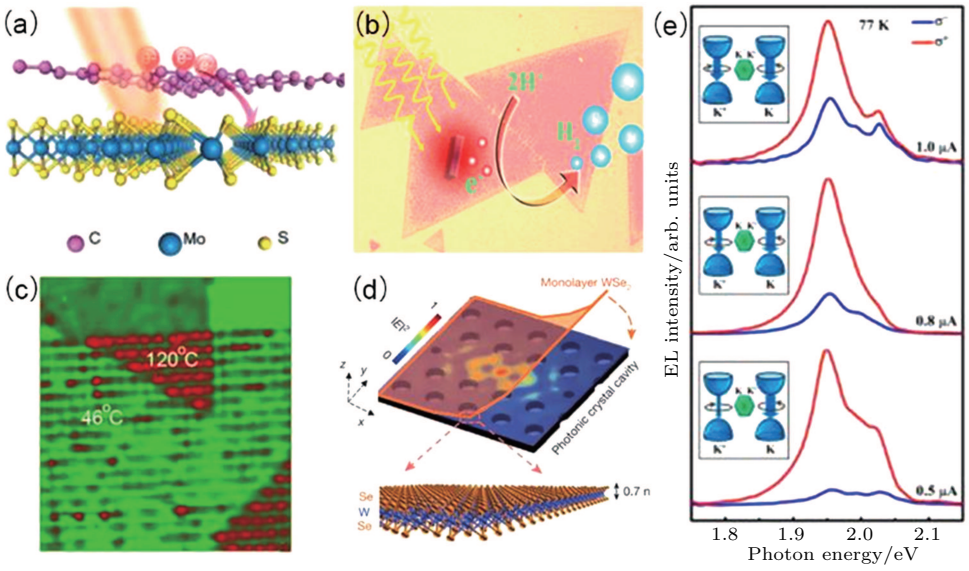


Fig. 8. (color online) Other device applications of 2D materials. (a) GQDs tuning MoS_2 luminescence.[80] (b) Plasmonic hot electrons enhanced MoS_2 photocatalysis.[81] (c) Plasmon-induced photo-thermo effect on MoS_2 monolayer.[82] (d) Photonic crystal microcavity pumping MoS_2 laser.[83] (e) Electrically controlled valley-LED device.[89]

showing a stable and reproducible laser device for practical applications. In addition, the strong light–matter interaction can be realized in a Bragger reflection photonic cavity with CVD-grown MoS_2. The angle-resolved spectra show a Rabi splitting of 46 ± 3 meV in reflectivity and PL spectra, which is arising from the coupling between MoS_2 exciton and cavity photons.[84]

TMDs monolayers possess two inequivalent valleys in the vicinity corner of the honeycomb Brillouin zone.[85,86] If the charge carriers can be confined and controlled in one of the specific valleys, the valleytronic device based on spin-valley coupling can be achieved.[87,88] As shown in Fig. 8(e), it is reported that the valley-LED device based on WS_2 monolayer can be modulated with gate tuning.[89] This fabricated device shows classical rectification properties because of the p–i–n heterostructure. By modulating the direction and amplitude of the forward bias current, valley polarization EL can be actively controlled. The EL emission among neutral exciton, trion, and bound exciton varies with switching electrostatic doping. This circularly EL can be understood that electrons of opposite spins occupy at K and K' valleys separately, and the largest degree of circular polarization was observed as high as 81% at 77 K. A series of valley emitting devices among TMDs have been widely researched by charge doping, selective optical excitation, and temperature-dependent tuning.

5. Conclusion and perspective

In conclusion, we have reviewed the state-of-the-art aspect of 2D materials among graphene, TMDs, and some hybrid structures. The optical properties of graphene and TMDs have been summarized, and the physical mechanism of light–matter interaction in these atomic thin materials has been elaborated. The plasmon-assisted devices based on 2D materials have been developed at a remarkable level for a wide variety of application fields, among light-emitting, photo-catalysis, and environmental-friendly energy. Although lots of intriguing physical phenomena and high performance devices have been observed and realized experimentally, exploiting the distinct advantages of 2D crystals and their superior devices is still full of challenges. In perspective, we propose several research directions for 2D materials of great importance, which are worth being discussed thoroughly in the future.

1) The quality of 2D materials 2D materials can be synthesized from several routes, including CVD growth, mechanical exfoliation, and solvothermal method. Each method has its own advantages and disadvantages, but the issues of common concern are the defects induced from inhomogenous growth and the impurities induced from the transfer process. For example, the sulfur vacancies existing in MoS_2 monolayer seriously influence the PL efficiency and electronic mobility. The graphene nanoribbon transistors with zig-zag and armchair edge may show different performance in electrical measurements.

2) The interface problem of 2D hybrid structures Hybrid structures based on 2D materials give enhanced optical signals and broad spectral photoresponse. However, the role of the interface between 2D material heterostructure and metal-2D semiconductor should be carefully discussed and systematically studied. The light–matter interaction of 2D heterostructures, such as carrier generation, charge transfer, and exciton coupling, occurs in the femtosecond timescale, which requires femtosecond pump-probe measurements to scrutinize their complicated physical phenomena. Charge transfer at a Schottky junction of a metal/2D semiconductor plays a significant role in optical and electronic measurements, and modulating the band structure and Fermi level of materials is paramount for studying the hot electrons doping effect.

3) The future device applications 2D materials are a big family with rapid development and innovation. In this review, graphene and TMDs are mainly discussed. Other novel 2D materials with growing attention, such as phosphorus and silylene, may provide even more possibility for functional applications in the future. However, for the prospects of commercialized production of 2D devices, it is still in an early stage. The reported 2D devices in the lab with distinct advantages and high performance have to face the challenge in the compatibility of large-scale CMOS integration at a low cost. In general, we are looking forward to the future of 2D materials, and expecting a great and prosperous time of 2D device applications.

References

[1] Novoselov K S, Geim A K, Morozov S V, Jiang D, Zhang Y, Dubonos S V, Grigorieva I V and Firsov A A 2004 *Science* **306** 666
[2] Butler S Z, Hollen S M, Cao L, Cui Y, Gupta J A, Gutierrez H R, Heinz T F, Hong S S, Huang J and Ismach A F 2013 *ACS Nano* **7** 2898
[3] Jones A M, Yu H, Ghimire N J, Wu S, Aivazian G, Ross J S, Zhao B, Yan J, Mandrus D G, Xiao D, Yao W and Xu X 2013 *Nat. Nanotech.* **8** 634
[4] Wang X, Gong Y, Shi G, Chow W L, Keyshar K, Ye G, Vajtai R, Lou J, Liu Z, Ringe E, Tay B K and Ajayan P M 2014 *ACS Nano* **8** 5125
[5] Yan K, Fu L, Peng H and Liu Z 2013 *Acc. Chem. Res.* **46** 2263
[6] Koppens F, Mueller T, Avouris P, Ferrari A, Vitiello M and Polini M 2014 *Nat. Nanotech.* **9** 780
[7] Wang W, Klots A, Prasai D, Yang Y, Bolotin K I and Valentine J 2015 *Nano Lett.* **15** 7440
[8] Liu Z, Ma L, Shi G, Zhou W, Gong Y, Lei S, Yang X, Zhang J, Yu J, Hackenberg K P, Babakhani A, Idrobo J C, Vajtai R, Lou J and Ajayan P M 2013 *Nat. Nanotech.* **8** 119
[9] Han D D, Zhang Y L, Jiang H B, Xia H, Feng J, Chen Q D, Xu H L and Sun H B 2015 *Adv. Mater.* **27** 332
[10] Lemme M C, Echtermeyer T J, Baus M and Kurz H 2007 *IEEE Electron Device Lett.* **28** 282
[11] Liao L, Lin Y C, Bao M, Cheng R, Bai J, Liu Y, Qu Y, Wang K L, Huang Y and Duan X 2010 *Nature* **467** 305
[12] Najmaei S, Liu Z, Zhou W, Zou X, Shi G, Lei S, Yakobson B I, Idrobo J C, Ajayan P M and Lou J 2013 *Nat. Mater.* **12** 754
[13] Splendiani A, Sun L, Zhang Y, Li T, Kim J, Chim C Y, Galli G and Wang F 2010 *Nano Lett.* **10** 1271

[14] Mak K F, Lee C, Hone J, Shan J and Heinz T F 2010 *Phys. Rev. Lett.* **105** 136805
[15] Mak K F, He K, Lee C, Lee G H, Hone J, Heinz T F and Shan J 2013 *Nat. Mater.* **12** 207
[16] Li Z, Xiao Y, Gong Y, Wang Z, Kang Y, Zu S, Ajayan P M, Nordlander P and Fang Z 2015 *ACS Nano* **9** 10158
[17] Lee C, Wei X, Kysar J W and Hone J 2008 *Science* **321** 385
[18] Hui Y Y, Liu X, Jie W, Chan N Y, Hao J, Hsu Y T, Li L J, Guo W and Lau S P 2013 *ACS Nano* **7** 7126
[19] He K, Poole C, Mak K F and Shan J 2013 *Nano Lett.* **13** 2931
[20] Ji J, Zhang A, Xia T, Gao P, Jie Y, Zhang Q and Zhang Q 2016 *Chin. Phys. B* **25** 077802
[21] Kim K S, Zhao Y, Jang H, Lee S Y, Kim J M, Kim K S, Ahn J H, Kim P, Choi J Y and Hong B H 2009 *Nature* **457** 706
[22] Lopez-Sanchez O, Lembke D, Kayci M, Radenovic A and Kis A 2013 *Nat. Nanotech.* **8** 497
[23] Zhang W, Chuu C P, Huang J K, Chen C H, Tsai M L, Chang Y H, Liang C T, Chen Y Z, Chueh Y L, He J H, Chou M Y and Li L J 2014 *Sci. Rep.* **4** 3826
[24] Casiraghi C, Hartschuh A, Lidorikis E, Qian H, Harutyunyan H, Gokus T, Novoselov K and Ferrari A 2007 *Nano Lett.* **7** 2711
[25] Blake P, Hill E, Neto A C, Novoselov K, Jiang D, Yang R, Booth T and Geim A 2007 *Appl. Phys. Lett.* **91** 063124
[26] Nair R R, Blake P, Grigorenko A N, Novoselov K S, Booth T J, Stauber T, Peres N M and Geim A K 2008 *Science* **320** 1308
[27] Lui C H, Mak K F, Shan J and Heinz T F 2010 *Phys. Rev. Lett.* **105** 127404
[28] Fang Z, Wang Y, Schlather A E, Liu Z, Ajayan P M, de Abajo F J, Nordlander P, Zhu X and Halas N J 2014 *Nano Lett.* **14** 299
[29] Fang Z, Thongrattanasiri S, Schlather A, Liu Z, Ma L, Wang Y, Ajayan P M, Nordlander P, Halas N J and García de Abajo F J 2013 *ACS Nano* **7** 2388
[30] Ayari A, Cobas E, Ogundadegbe O and Fuhrer M S 2007 *J. Appl. Phys.* **101** 14507
[31] Ross J S, Wu S, Yu H, Ghimire N J, Jones A M, Aivazian G, Yan J, Mandrus D G, Xiao D, Yao W and Xu X 2013 *Nat. Commun.* **4** 1474
[32] Lin Y, Ling X, Yu L, Huang S, Hsu A L, Lee Y H, Kong J, Dresselhaus M S and Palacios T 2014 *Nano Lett.* **14** 5569
[33] Dhakal K P, Duong D L, Lee J, Nam H, Kim M, Kan M, Lee Y H and Kim J 2014 *Nanoscale* **6** 13028
[34] Korn T, Heydrich S, Hirmer M, Schmutzler J and Schuller C 2011 *Appl. Phys. Lett.* **99** 102109
[35] Lazzeri M, Piscanec S, Mauri F, Ferrari A and Robertson J 2005 *Phys. Rev. Lett.* **95** 236802
[36] Kampfrath T, Perfetti L, Schapper F, Frischkorn C and Wolf M 2005 *Phys. Rev. Lett.* **95** 187403
[37] Ye R, Xiang C, Lin J, Peng Z, Huang K, Yan Z, Cook N P, Samuel E L, Hwang C C, Ruan G, Ceriotti G, Raji A R, Marti A A and Tour J M 2013 *Nat. Commun.* **4** 2943
[38] Gokus T, Nair R, Bonetti A, Bohmler M, Lombardo A, Novoselov K, Geim A, Ferrari A and Hartschuh A 2009 *ACS Nano* **3** 3963
[39] Lu J, Yang J X, Wang J, Lim A, Wang S and Loh K P 2009 *ACS Nano* **3** 2367
[40] Ye R, Peng Z, Metzger A, Lin J, Mann J A, Huang K, Xiang C, Fan X, Samuel E L, Alemany L B, Marti A A and Tour J M 2015 *ACS Appl. Mater. Interfaces* **7** 7041
[41] Li L, Wu G, Yang G, Peng J, Zhao J and Zhu J J 2013 *Nanoscale* **5** 4015
[42] Korn T, Heydrich S, Hirmer M, Schmutzler J and Schüller C 2011 *Appl. Phys. Lett.* **99** 102109
[43] Newaz A, Prasai D, Ziegler J, Caudel D, Robinson S, Haglund Jr R and Bolotin K 2013 *Solid State Commun.* **155** 49
[44] Nan H, Wang Z, Wang W, Liang Z, Lu Y, Chen Q, He D, Tan P, Miao F and Wang X 2014 *ACS Nano* **8** 5738
[45] Mouri S, Miyauchi Y and Matsuda K 2013 *Nano Lett.* **13** 5944
[46] Fang Z and Zhu X 2013 *Adv. Mater.* **25** 3840
[47] Fang Z, Wang Y, Liu Z, Schlather A, Ajayan P M, Koppens F H, Nordlander P and Halas N J 2012 *ACS Nano* **6** 10222
[48] Jiang R, Li B, Fang C and Wang J 2014 *Adv. Mater.* **26** 5274
[49] Atwater H A and Polman A 2010 *Nat. Mater.* **9** 205
[50] Huang T, Wang J, Li Z, Liu W, Lin F, Fang Z and Zhu X 2016 *Chin. Phys. B* **25** 087302
[51] Zhang Y and Wang X 2015 *Chin. Phys. B* **24** 057301
[52] Chen J, Badioli M, Alonso-Gonzalez P, Thongrattanasiri S, Huth F, Osmond J, Spasenovic M, Centeno A, Pesquera A, Godignon P, Elorza A Z, Camara N, Garcia de Abajo F J, Hillenbrand R and Koppens F H 2012 *Nature* **487** 77
[53] Boltasseva A and Atwater H A 2011 *Science* **331** 290
[54] Wang Y, Ou J Z, Chrimes A F, Carey B J, Daeneke T, Alsaif M M, Mortazavi M, Zhuiykov S, Medhekar N, Bhaskaran M, Friend J R, Strano M S and Kalantar-Zadeh K 2015 *Nano Lett.* **15** 883
[55] Atwater H A and Polman A 2010 *Nat. Phys.* **9** 205
[56] Xu D, Wang X, Huang Y, Ouyang S, He H and He H 2015 *Chin. Phys. B* **24** 024205
[57] Giannini V, Fernández-Domínguez A I, Sonnefraud Y, Roschuk T, Fernández-García R and Maier S A 2010 *Small* **22** 2498
[58] Yu Y, Ji Z, Zu S, Du B, Kang Y, Li Z, Zhou Z, Shi K and Fang Z 2016 *Adv. Funct. Mater.* **26** 6394
[59] Kang Y, Najmaei S, Liu Z, Bao Y, Wang Y, Zhu X, Halas N J, Nordlander P, Ajayan P M and Lou J 2014 *Adv. Mater.* **26** 6467
[60] Liu W, Lee B, Naylor C H, Ee H S, Park J, Johnson A T C and Agarwal R 2016 *Nano Lett.* **16** 1262
[61] Wang S, Li S, Chervy T, Shalabney A, Azzini S, Orgiu E, Hutchison J A, Genet C, Samorì P and Ebbesen T W 2016 *Nano Lett.* **16** 4368
[62] Zu S, Li B, Gong Y, Li Z, Ajayan P M and Fang Z 2016 *Adv. Func. Mater.*
[63] Wang Z, Dong Z, Gu Y, Chang Y H, Zhang L, Li L J, Zhao W, Eda G, Zhang W, Grinblat G, Maier S A, Yang J K, Qiu C W and Wee A T 2016 *Nat. Commun.* **7** 11283
[64] Akselrod G M, Ming T, Argyropoulos C, Hoang T B, Lin Y, Ling X, Smith D R, Kong J and Mikkelsen M H 2015 *Nano Lett.* **15** 3578
[65] Luk'yanchuk B, Zheludev N I, Maier S A, Halas N J, Nordlander P, Giessen H and Chong C T 2010 *Nat. Mater.* **9** 707
[66] Huang M, Chen D, Zhang L and Zhou J 2016 *Chin. Phys. B* **25** 057303
[67] Lee B, Park J, Han G H, Ee H S, Naylor C H, Liu W, Johnson A C and Agarwal R 2015 *Nano Lett.* **15** 3646
[68] Fang Z, Liu Z, Wang Y, Ajayan P M, Nordlander P and Halas N J 2012 *Nano Lett.* **12** 3808
[69] Echtermeyer T, Britnell L, Jasnos P, Lombardo A, Gorbachev R, Grigorenko A, Geim A, Ferrari A and Novoselov K 2011 *Nat. Commun.* **2** 458
[70] Britnell L, Ribeiro R, Eckmann A, Jalil R, Belle B, Mishchenko A, Kim Y J, Gorbachev R, Georgiou T and Morozov S 2013 *Science* **340** 1311
[71] Miao J, Hu W, Jing Y, Luo W, Liao L, Pan A, Wu S, Cheng J, Chen X and Lu W 2015 *Small* **11** 2392
[72] Yu S H, Lee Y, Jang S K, Kang J, Jeon J, Lee C, Lee J Y, Kim H, Hwang E and Lee S 2014 *ACS Nano* **8** 8285
[73] Pak J, Jang J, Cho K, Kim T Y, Kim J K, Song Y, Hong W K, Min M, Lee H and Lee T 2015 *Nanoscale* **7** 18780
[74] Eginligil M, Cao B, Wang Z, Shen X, Cong C, Shang J, Soci C and Yu T 2015 *Nat. Commun.* **6** 7636
[75] Hong X, Kim J, Shi S F, Zhang Y, Jin C, Sun Y, Tongay S, Wu J, Zhang Y and Wang F 2014 *Nat. Nanotech.* **9** 682
[76] He J, Kumar N, Bellus M Z, Chiu H Y, He D, Wang Y and Zhao H 2014 *Nat. Commun.* **5** 5622
[77] Rivera P, Schaibley J R, Jones A M, Ross J S, Wu S, Aivazian G, Klement P, Seyler K, Clark G, Ghimire N J, Yan J, Mandrus D G, Yao W and Xu X 2015 *Nat. Commun.* **6** 6242
[78] Lauchner A, Schlather A E, Manjavacas A, Cui Y, McClain M J, Stec G J, García de Abajo F J, Nordlander P and Halas N J 2015 *Nano Lett.* **15** 6208
[79] Manjavacas A, Marchesin F, Thongrattanasiri S, Koval P, Nordlander P, Sanchez-Portal D and Garciía de Abajo F J 2013 *ACS Nano* **7** 3635
[80] Li Z, Ye R, Feng R, Kang Y, Zhu X, Tour J M and Fang Z 2015 *Adv. Mater.* **27** 5235
[81] Kang Y, Gong Y, Hu Z, Li Z, Qiu Z, Zhu X, Ajayan P M and Fang Z 2015 *Nanoscale* **7** 4482
[82] Najmaei S, Mlayah A, Arbouet A, Girard C, Léotin J and Lou J 2014 *ACS Nano* **8** 12682
[83] Wu S, Buckley S, Schaibley J R, Feng L, Yan J, Mandrus D G, Hatami F, Yao W, Vuckovic J, Majumdar A and Xu X 2015 *Nature* **520** 69
[84] Liu X, Galfsky T, Sun Z, Xia F, Lin E, Kéna-Cohen S and Menon V M 2014 *Nat. Photon.* **9** 30
[85] Yu T and Wu M W 2014 *Phys. Rev. B* **89** 205436
[86] Mak K F, He K, Shan J and Heinz T F 2012 *Nat. Nanotech.* **7** 494
[87] Xu X, Yao W, Xiao D and Heinz T F 2014 *Nat. Phys.* **10** 343
[88] Mak K F, McGill K L, Park J and McEuen P L 2014 *Science* **344** 1489
[89] Yang W, Shang J, Wang J, Shen X, Cao B, Peimyoo N, Zou C, Chen Y, Wang Y, Cong C, Huang W and Yu T 2016 *Nano Lett.* **16** 1560